Int. J. Heat Mass Transfer. Vol. 31, No. 7, pp. 1375–1384, 1988
Printed in Great Britain

0017 9310/88 $3.00 + 0.00

Full-field *in situ* measurement of local mass transfer coefficient using ESPI with the swollen polymer technique

C. L. SALUJA, B. L. BUTTON and B. N. DOBBINS
Mechanical Engineering Department, Trent Polytechnic, Burton Street, Nottingham NG1 4BU, U.K.

(*Received* 28 *September* 1987 *and in final form* 3 *December* 1987)

Abstract—A novel experimental arrangement for *in situ* measurement of the local mass transfer coefficient using a right-angle glass prism with an electronic speckle pattern interferometer and the swollen polymer technique is described. The viability of the arrangement in providing the mass transfer data is demonstrated by considering the case of a laminar air jet impinging on a flat surface. The measured data are found to agree with the available theoretical predictions to within the order of the experimental uncertainty. Practical recommendations for reducing this uncertainty are also made.

INTRODUCTION

A WIDE variety of techniques has been used for the determination of overall or local heat transfer coefficients for engineering components [1]. These can be divided into two categories; direct measurement techniques which are based on determination of temperature and heat flux on a test surface and indirect measurement techniques which are usually based on the determination of mass transfer coefficients using a suitable mass transfer technique and invoking of an analogy between heat and mass transfer, e.g. that of Chilton and Colburn [2]. One class of mass transfer techniques relies on the profilometric determination of the change in surface height caused by mass transfer from the surface. The 'swollen polymer mass transfer technique', pioneered by Dr N. Macleod of Edinburgh University, belongs to this class and has been in use for about the last 15 years. The technique utilizes the swelling properties of silicone rubbers which swell reversibly under the action of suitable swelling agents, typically esters. A layer of the polymer is cast on a test surface and swollen in the organic fluid. Under the influence of an experimental fluid flow, the swelling fluid evaporates and the thickness of the polymer changes. The change in the thickness of the polymer at a location on the test surface is a measure of the mass of the swelling fluid that has evaporated provided the duration of the test satisfies specific criteria. From the mass loss the local mass transfer coefficient can be determined and hence the heat transfer coefficient can be estimated.

The swollen polymer technique offers several advantages over the widely used naphthalene sublimation techniques, e.g. the one used in ref. [3]. The polymer coating does not require recasting after each test as it can be reactivated simply by soaking in the swelling agent for a few hours; the changes in surface height due to mass transfer can be kept to the order of a few micrometres and hence are too small to affect the fluid flow under investigation; also the optical quality of the test surface is such that interferometry can be used.

The swollen polymer technique has been used in conjunction with a variety of interferometric techniques to record the change of thickness of the polymer coating. Measurements can be made either *in situ* or with separate test and optical facilities. For *in situ* measurements, the swollen polymer test coating is exposed to the experimental mass transferring fluid flow without being moved from the optical arrangement used to measure recession. Alternatively, optical measurements are carried out using an interferometer remote from the mass transfer test facility. This requires the test surface to be moved between the two activities. Although the latter approach is more convenient to use and helps to overcome the vibration isolation problem encountered with *in situ* measurements, it suffers from the problem that the temperature of the polymer coating and its substrate during measurement can be substantially different to that existing during its exposure to the experimental fluid. This can make accurate interpretation of the resulting fringe pattern difficult as the effect of the variation of temperatures on the substrate thickness cannot be isolated from configurational changes on the polymer surface due to mass transfer. In the former approach, the presence of temperature effects can be completely eliminated simply by ensuring a constant ambient temperature in the area of mass transfer experiments and maintaining the mass transferring fluid at the same temperature. This approach also improves the speed of data acquisition and eases the problem of ordinal number assignment to the fringes of the patterns resulting from the interferometric technique used. Hence, the *in situ* measurement approach has

NOMENCLATURE

C	concentration
d	nozzle diameter
D	diffusivity
F	final optical path length
Fm	exterior momentum flux
$[-g'(0)]$	function of Schmidt number (see equation (7))
h_m	local mass transfer coefficient
i	angle of incidence (see Fig. 5)
I	initial optical path length
l	length parameter, used to satisfy boundary conditions at $r = 0$ on polymer coating surface
n	fringe order number
P	pressure
Px	pitch of impingement nozzles in X-direction
Py	pitch of impingement nozzles in Y-direction
Q	air flow rate
r	radial distance from impingement jet axis on polymer coating surface
Re	Reynolds number
Sc	Schmidt number
Sh	Sherwood number
t	time of exposure of jet to polymer surface from the instance of refreshing a reference frame in the frame store unit
u	impingement jet velocity
x	distance along horizontal axis on polymer coating surface
y	distance along vertical axis on polymer coating surface.

Greek symbols

α	complement of angle of incidence or of reflection at polymer–air interface (see Fig. 5)
δ	recession of polymer coating (see Fig. 5)
η	refractive index
λ	wavelength of light
ν	kinematic viscosity
ρ	density
ϕ	angle of refraction or of incidence at polymer–glass interface (see Fig. 5)
Ψ	defined in equation (9).

Subscripts

A	ambient air
e	estimated value
g	glass
p	polymer
pc	plenum chamber
ref	reference point
S.A.	swelling agent.

Superscript

$\bar{}$	mean value.

greater potential utility. One such arrangement for recession measurements of the polymer coating in conjunction with an electronic speckle pattern interferometer is described here. Also, the soundness and limitations of the arrangement are demonstrated by considering the case of a laminar jet impinging on a flat surface.

PREVIOUS WORK

The swollen polymer technique was first described by Macleod and Todd [4] who also put forward considerations for the suitable choice of the polymer–swelling agent system and for the operating conditions. They used a combined pneumatic and electromagnetic gauge for the measurement of local polymer thickness changes and the weight loss of a removable section of the test surface of the swollen polymer for average thickness changes.

Kapur and Macleod [5, 6] employed the swollen polymer technique for the study of various jet impingement and convective fluid flow situations. They used double exposure holographic interferometry to measure the changes in thickness of the polymer. In each of their tests, the experimental surface was presented to a laser holographic set-up first before and then after mass transfer. Both the holographic exposures were recorded on the same holographic plate and reconstruction of an image from the plate generated an interference pattern. The pattern was a complete record of the polymer thickness changes and hence, of the local variation of mass transfer coefficient over the entire test surface.

Masliyah and Nguyen [7] investigated free convection from a vertical plate by measuring the weight loss of a swelling agent from a polymer film when it was exposed to a bath of water. The same authors [8, 9] also used double exposure frozen fringe holographic interferometry to study mass transfer due to impinging square, and rectangular jets.

To translate information on a frozen interference pattern into absolute values of mass transfer coefficients requires the identification of the ordinal number of the fringes. This task is relatively simple for the case of an impinging jet but for cases of flow situations which result in a number of maxima and minima or other complicated fringe patterns, the task is formidable and poses serious limitation on the use of the technique. For the study of the variation of the analogous heat transfer coefficient on a film-cooled

surface, Saluja *et al.* [10] also used double exposure laser holographic interferometry with the swollen polymer but to facilitate fringe identification, air gauges were used.

With a view to easing fringe identification and differentiation of maxima and minima in an interference pattern, Harper and Macleod [11] described an arrangement in which interference fringes could be observed in real time. In their arrangement, a record of the initial state of the polymer surface is first made on a holographic plate which is then processed. Subsequently, mass transfer is allowed to take place from the polymer surface while the surface also forms a part of the holographic set-up. A fringe pattern becomes evident when the test specimen is viewed through the holographic plate. Using an arrangement similar to that of Harper and Macleod, Law and Masliyah [12] studied mass transfer due to an impinging confined laminar two-dimensional air jet on a flat surface.

The technique of live holographic interferometry employed by various researchers mentioned above, is a photographic one. It involves time consuming processing of photographic plates and requires a skilled operator. Non-photographic interferometers which do away with the photographic plate and hence its processing, have recently been made commercially available and these can be used with the swollen polymer technique. One such interferometer (made by Vinten Limited, Bury St. Edmunds, U.K.) uses the speckle effect and was used by Hyne and Macleod [13] for the study of mass transfer due to a turbulent jet impinging on a flat plate.

In the experimental set-up employed by Hyne and Macleod, the object beam from the interferometer illuminating the test surface and scattered beam from the surface were on the same side as the impingement jet tube. The presence of the jet tube on the same side as the beams led to a loss of information from a part of the test surface.

In the experimental arrangement described in this paper, the swollen polymer technique is used in conjunction with the electronic speckle pattern interferometer of Vinten Limited but the shortcoming of Hyne and Macleod is overcome by using an adaptation of the total internal reflection technique previously described by Harper and Macleod. In this the impinging jet is on one side of the coated test surface and both the illuminating and scattered beams are on the other side. The arrangement provides a full-field view of the test surface. Harper and Macleod suggested the use of holographic interferometry to yield absolute values of recession and hence, of mass or analogous heat transfer data on the test surface. The novel aspect of the present arrangement lies in the use of an electronic speckle interferometer for the recession measurements.

To demonstrate the viability of the arrangement in providing the mass transfer data, tests were conducted using an axisymmetric laminar jet impinging on a flat surface and the results of these are reported here.

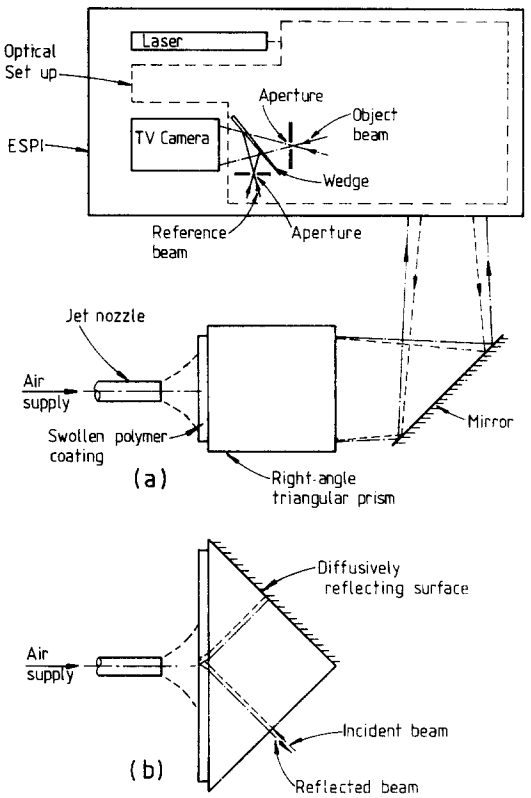

FIG. 1. Experimental arrangement: (a) top view; (b) front view (part view).

EXPERIMENTAL ARRANGEMENT

In the arrangement described in this work, an electronic speckle pattern interferometer is employed to record thickness changes on a swollen polymer coated test surface. The interferometer records and manipulates electronically the speckle pattern generated by the scattering of a laser beam from a diffusively reflecting experimental surface. The scattered beam is combined with a reference beam and the resulting speckle interference pattern can be seen on a VDU. An initial record of the interference pattern is stored and is subtracted automatically from subsequent live patterns from the experimental surface to yield fringe patterns. The fringe patterns can be monitored in real time and simultaneously recorded on a video cassette for image processing at a later stage.

It may, however, be pointed out that the fringe patterns produced by this technique are not as distinct as obtained by the holographic interferometric technique.

Figure 1 depicts the experimental arrangement consisting of an electronic speckle pattern interferometer, a right-angle glass prism and an impingement nozzle. The arrangement of optical components of the interferometer is very similar to the one described by Jones and Wykes [14].

In the experimental arrangement, a flat test surface is formed by coating the hypotenuse (204×204 mm)

of the right-angle prism to a thickness of about 0.5 mm. The prism is held with the hypotenuse vertical and its two inclined faces are at 45° to the horizontal plane. The output mirror of the interferometer is adjusted such that the object beam is incident normal to the lower inclined surface of the prism, at about its centre. The object beam is refracted at the glass–polymer interface and is then totally internally reflected at the polymer–air interface. Then after refraction at the polymer–glass interface again it falls nearly normal to the upper inclined diffusively reflecting surface of the prism. The upper surface of the prism is sprayed with Zyglo developer (SKD-NF/ZP.9, made by Magnaflux Limited, Swindon, U.K.). On drying for about 5 min, the developer provides a diffusively reflecting white surface. The beam scattered by the surface passes back through the glass prism along a path similar to that of the illuminating beam. After being reflected by a number of mirrors, it passes through an adjustable aperture and then through a lens which focuses the beam through a wedge onto a TV camera faceplate.

A part of the main laser beam forms a reference beam for the interferometer. After being reflected by a number of mirrors and prisms, the beam passes through two lenses and an aperture. Finally it is combined with the object beam at the wedge mentioned above to generate an interference pattern.

The TV camera tube, in front of which the interference pattern is located, can be moved in or out to produce a sharp image on a TV monitor. The interference pattern which is due to the speckle effect as the main beam is scattered from the upper inclined surface of the prism, consists of dark and bright spots or speckles. The size of the speckles can be adjusted by varying the size of the aperture through which the main beam passes. If the aperture is increased, the size of the speckles is reduced and vice versa. The speckle size is suitably adjusted so that the fringe contrast is maximized.

The arrangement of the electronic equipment used for monitoring and recording interference patterns is shown in Fig. 2. The TV camera transmits the interference pattern to a frame memory unit (FM 60, made by FOR.A Co. Ltd., Japan and modified at Loughborough University, Loughborough, U.K.) from which the signal can either be sent to a TV monitor or it could be stored in its memory. The stored signal can be automatically subtracted from subsequent signals coming from the TV camera. The subtracted images are recorded on a magnetic tape in a video cassette recorder. Later on, the information is played back on the TV monitor to analyse it.

EXPERIMENTATION

Using the arrangement described above, tests were conducted using a nozzle with an exit diameter of 6.48 mm. Figure 3 shows the design of the nozzle used and it is similar to the one used by Gardon and

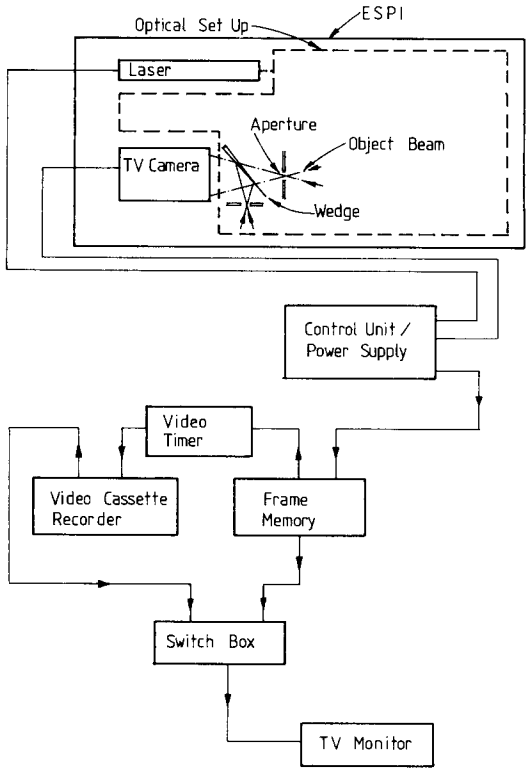

FIG. 2. Arrangement of electronic equipment used with the ESPI.

Cobonpue [15]. The tests were for two Reynolds numbers (based on nozzle diameter) of 1328 and 1319. With the Reynolds numbers used, the impingement jet in each case was laminar. Also the nozzle diameter to flat test surface spacing was 1.0 in each test.

The arrangement used for the supply of air to the nozzle is shown in Fig. 4. The air was supplied at a pressure of about 5 bar. After being filtered and metered, it was sent to a Perspex plenum chamber (240 × 240 × 150 mm). To one of the vertical faces of the plenum chamber, the nozzle was screwed in and it was adjusted so that the nozzle axis was normal to the vertical polymer test surface. The base of the plenum chamber was mounted on a traverse mechanism so that the nozzle to coated test surface spacing could be varied. The traverse mechanism was bolted rigidly to a 900 × 1500 × 800 mm top of cast iron on

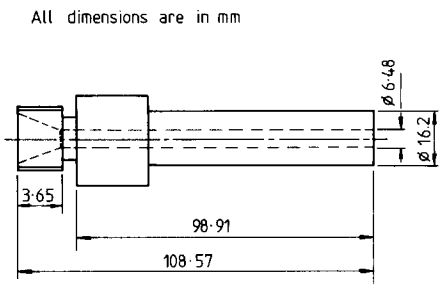

FIG. 3. Details of impinging jet nozzle.

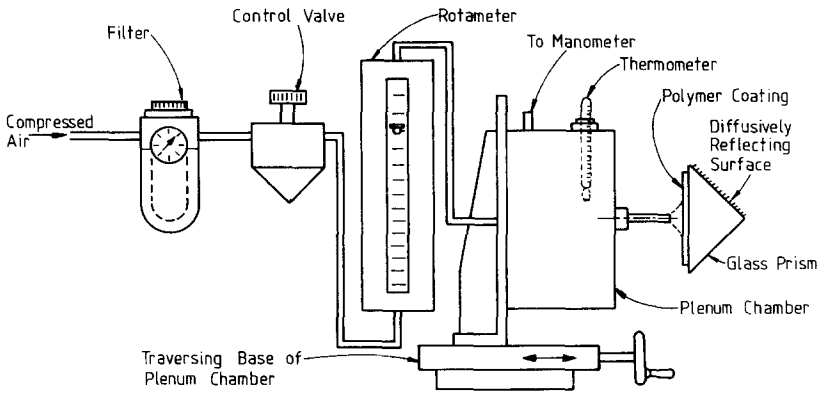

FIG. 4. Arrangement for the supply of air to the impinging nozzle.

a concrete table which was supported on four pressurized air bellows to provide isolation from ground-borne vibrations. The base of the interferometer containing the laser, the TV camera and the optical set-up including the right-angle prism with polymer coated hypotenuse, shown in Fig. 1, also rested on the table.

Before conducting actual tests, the prism with the polymer coating which had been soaking in a swelling agent, was removed from its bath and installed as shown in Fig. 1 and its surface was dried by using a lint free paper. Care was taken to ensure that the lower optical face of the prism remained uncontaminated. A square grid marked at suitable spacing on a white card was then placed on the upper inclined face of the prism and its focused image, as seen by the TV camera, was recorded on a video tape for spatial calibration. The size of the viewing aperture and reference beam attenuation were adjusted to obtain optimum contrast.

Having removed the calibration grid, the upper inclined surface of the glass prism was sprayed with Zyglo developer. The nozzle was adjusted to the required distance from the polymer coated surface of the prism. The air supply to the plenum chamber was switched on and its flow rate, measured using a rotameter, was adjusted to give the desired jet Reynolds number. During this operation the coated surface was protected by holding a piece of cardboard between it and the nozzle exit. The test period commenced with the removal of the piece of cardboard from the front of the nozzle exit. The image of the speckle pattern formed by the test surface was then recorded in the frame memory by selecting the subtraction mode of operation and depressing the 'store' button. As the mass transfer proceeded, the subtracted images were recorded on a video tape. When the fringes close to the centre of the jet were too many to be resolved, the stored image was refreshed by depressing the 'store' button again. The fringes displayed showed change of polymer coating thickness from the new reference position. During a run, the stored image was refreshed about four times and the interference fringes were recorded.

ANALYSIS OF DATA

Using a calibration equation of the rotameter, the Reynolds number of the jet issuing out of the nozzle was calculated taking into consideration the temperatures and pressures at the times of calibration and experimentation.

Figure 5 illustrates the relationship between the change in optical path length and the change in normal thickness of the polymer coating. In this figure, X′AHBDCY′ depicts the initial path of the laser beam passing through the prism and the polymer coating. The final path of the beam is X″EDCY′ after the coating has undergone a uniform recession of δ. It is assumed that the scattered light from the sprayed surface returns along the incident path to the camera

I, Initial total path length through the prism and polymer $= 2(X'Y') = 2[\eta_g(X'A+CY')+\eta_p(AB+BC)]$

F, Final total path length through the prism and polymer $= 2(X''Y')$

$$= 2[\eta_g(X''G+EG+CY')+\eta_p(ED+CD)].$$

It can be shown that

$$\text{Change in path length} = [I-F] = (4\delta/\cos\phi_1)[\eta_p-\eta_g^2/\eta_p\sin^2(i_1)].$$

The presence of a fringe in the interference pattern is due to a change in optical path of $\lambda/2$ where λ denotes the wavelength of the laser light used. If n is the order of a fringe on the fringe pattern, we have

$$\text{Change in path length} = (4\delta/\cos\phi_1)[\eta_p-\eta_g^2/\eta_p\sin^2(i_1)] = n\lambda/2.$$

Using

$$i_1 = 45^\circ$$

$$\eta_g = 1.518$$

$$\eta_p = 1.429$$

and

$$\lambda = 632.8\ \text{nm}$$

we have

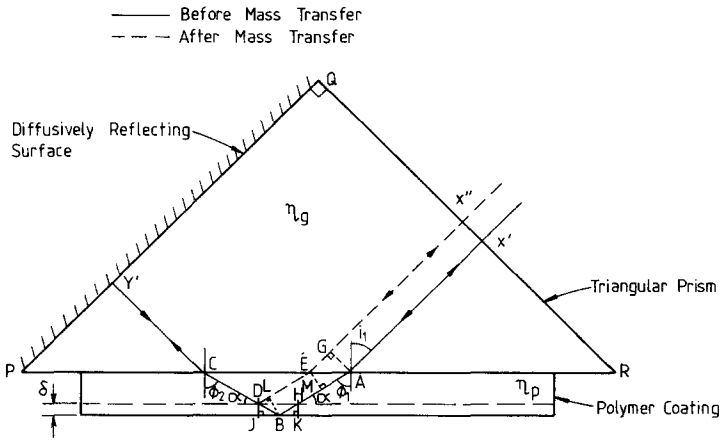

FIG. 5. Path of light through prism and polymer coating.

$$d\delta/dt = 0.08385 \times 10^{-6}(dn/dt).$$

If the experiment is conducted within the 'constant rate period' for which recession, δ, is linearly related to time, t, of experimentation, we have

$$\delta/t = 0.08385 \times 10^{-6}(dn/dt). \quad (1)$$

For a run, the fringe velocity, dn/dt, was obtained by analysis of interference fringes on the video tape. Initially the spatial calibration grid was used to produce scales for the principal axes on the interference fringe pattern. The centre of the impingement jet and a reference point a suitable location from the centre were marked on the TV monitor. The video tape of the recorded fringes was brought to the start of a fresh take at which instant a reference fringe pattern was recorded. The tape of the recorded fringes was then played and using a programme on a BBC microcomputer, the times of passing of the likely mid-points and definite end points of fringes past the marked reference point were noted. For each take of the recorded fringes, the timing was repeated five times and all the takes within a run were considered in this way.

For each set of readings, the fringe number, n, was plotted against the time, t, of passing of the likely mid-points of the fringes. Two typical plots are shown in Fig. 6. All the plots for a run were straight lines, the values of their slope were the same to within 5% and showed no systematic variation. This confirmed that the experiments were conducted within the constant rate period. The 'constant rate period' is defined by Macleod and Todd [4] as a period within which the vapour pressure of the swelling agent over the polymer surface does not drop below 95% of its saturation value. Under this condition the evaporation of the swelling agent is controlled predominantly by the air-side convective mass transfer coefficient and no significant concentration gradient or resistance to diffusion of the swelling agent to the polymer surface occurs within the polymer. The slopes of the plots gave dn/dt and the various values of these for a run were averaged and used in equation (1) to give δ/t.

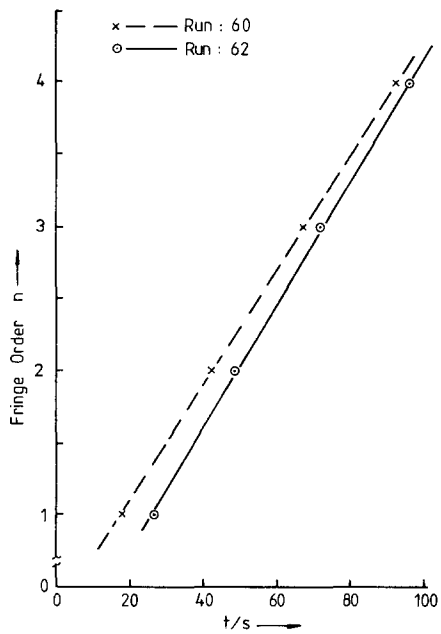

FIG. 6. Typical plots of n vs t.

The coefficient of mass transfer, h_m, was calculated using the following equation given by Macleod and Todd:

$$\delta/t = h_m C_s/\rho_{S.A.} \quad (2)$$

where C_s is the concentration of the swelling agent used and $\rho_{S.A.}$ the density of the swelling agent. In equation (2) it is assumed that saturated vapours of the swelling agent exist close to the swollen polymer surface during mass transfer. The value of saturation vapour pressure required for the calculation of C_s was calculated using the following empirical equation obtained from the data of Paterson *et al.* [16]:

$$\log p(\text{mm Hg}) = 8.887 - 3005.49/T. \quad (3)$$

To obtain the spatial variation of the mass transfer, a fringe pattern at a time t from the moment or refresh-

ing of the reference stored image was frozen on the TV monitor and the locations at which various fringes intersected the X- and Y-axes were noted. By ensuring that there was a fringe at the reference location at which fringe velocity was determined previously, it was possible to obtain the absolute value of the fringe order on the fringe pattern. The absolute fringe order number of the other fringes was obtained by inspection of the video record to obtain the direction of travel of the fringes. The mass transfer coefficient, h_m, at a point on a fringe with ordinal number of n was calculated using the following equation:

$$h_m/h_{m,\mathrm{ref}} = n/n_{\mathrm{ref}}.$$

RESULTS AND DISCUSSION

A typical fringe pattern obtained during the work here is shown in Fig. 7. As can be seen, each fringe is elliptical. This is due to the different spatial calibration factors in the horizontal and vertical planes; when viewing through the prism, these are in the ratio $\sqrt{2}:1$. Each fringe on the pattern represents a contour of constant recession and hence, of constant mass transfer coefficient. Spatial calibration of the image was determined by examination of the calibration grid and hence any point on the image could be related to a corresponding point on the test surface. On playing back the recorded interference fringe patterns, it was evident, since the fringes moved outwards as a run proceeded, the order of fringes on a frozen fringe pattern increased towards the centre of the impinging jet. The quality of fringes was not found to be very good and over a region with $r/d < 2$, the fringes were not distinguishable. For each fringe on the frozen fringe pattern, the four points at which each fringe intersected the horizontal and vertical axes X and Y, were considered. The radial distribution of mass transfer coefficient was obtained in this manner. The values of the mass transfer coefficient were also determined from the theory of Scholtz and Trass [17]. For these calculations the solution given by the authors, with approximations for the case of a radial wall jet with Sc between 1 and 4000, was not used directly. Instead, the exact solution of the momentum equation obtained by Glauert [18], under the assumption of the self-preserving boundary layer, was used and it is given by

$$h_m = 1.433D[Fm/\nu^3]^{1/4}[-g'(0)]x^{-5/4}[1+(l/r)^3]^{-0.75} \quad (4)$$

where Fm represents exterior momentum flux. It was shown by Glauert to be a constant and independent of radial position. Assuming that momentum of the jet was not affected by it being deflected by the plate, Fm was replaced by its estimated value, Fm_e, given by

$$Fm_e = \bar{u}^3 d^4/128. \quad (5)$$

The length parameter l in equation (4) was introduced by Glauert to allow for the fact that in a practical case

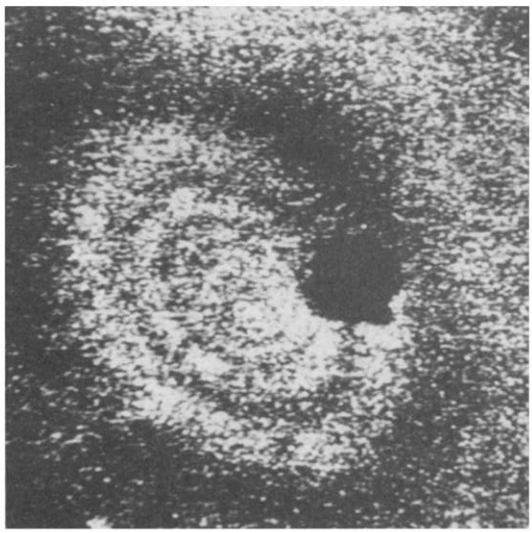

FIG. 7. Fringe pattern showing contours of equal mass transfer coefficient due to an impinging laminar jet ($Re = 1328$, $d = 6.48$ mm, $z/d = 1.0$).

of a wall jet, the assumed boundary conditions were not satisfied at the jet stagnation point $r = 0$. Following the suggestion by Schwartz and Caswell [19], l was replaced by its estimated value, l_e, obtained by equating the volumetric flux in the wall at $r = 0$ to that in the nozzle and is given by

$$l_e/d = 0.1327Re^{1/3}. \quad (6)$$

Also, the term $[-g'(0)]$ in equation (4) was given by

$$[-g'(0)] = (Sc+1/3)/Sc^{1/3}. \quad (7)$$

Using equations (5) and (6), equation (4) reduces to

$$h_m = 0.4260(D/r)Re^{3/4}[-g'(0)](d/r)^{1.4}\Psi \quad (8)$$

where

$$\Psi = [1+2.337\times10^{-3}Re(d/r)^3]^{0.75}. \quad (9)$$

The mass transfer coefficients predicted by equation (8) were computed using the values of the diffusivity, D, given by Reid and Sherwood [20]. Taking into consideration the assumptions made in the derivation of equation (8) and the uncertainty of the parameters involved in it, it is estimated that the uncertainty associated with the predicted data is $\pm 10.6\%$. The uncertainty associated with the value of diffusivity was calculated from the kinetic theory and it did not include any allowance for the unknown uncertainties in the empirical constants.

The experimental and predicted data are shown in Fig. 8. It can be seen that most of the experimental values for run No. 60 are lower than the predicted values, although there are some points at low values of r/d which are in close agreement. For the run, a mean curve drawn through the experimental results differs by as much as 25% at higher values of r/d. For run No. 62, the experimental results are in much better agreement with the theoretically predicted values of

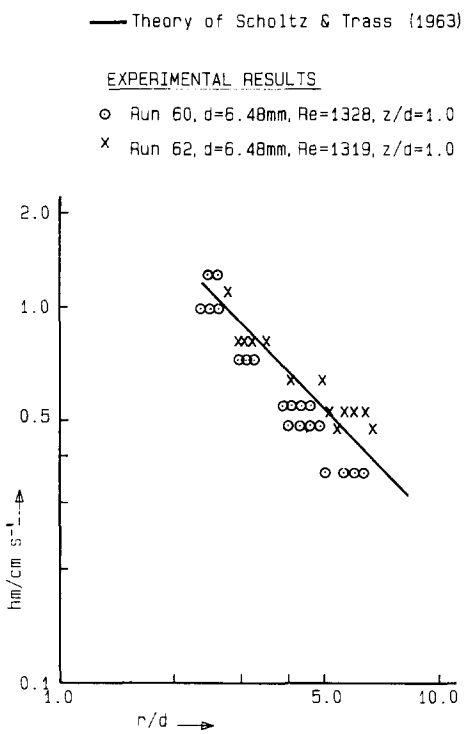

FIG. 8. Radial variation of mass transfer coefficients due to a laminar impinging jet.

Scholtz and Trass. Looking at the experimental data due to the two runs, it can also be inferred that the experimental arrangement did not offer good repeatability of results. The authors feel that the lack of complete vibration isolation of the working table which was found to be very difficult to achieve, and the adoption of a tedious manual fringe analysis procedure were partly responsible for the observed effect.

During the experimental work, all major sources of error were noted. An error analysis was carried out following the method of Kline and McClintock [21]. This indicated an uncertainty of $\pm 26.5\%$ in the values of h_m and $\pm 3.77\%$ in the values of Re. The large uncertainties in the values of h_m are due to large uncertainty in the values of the saturation vapour pressure. For ethyl salicylate which was the swelling agent used in the present work, the vapour pressure measurements available in the literature are due to Kapur and Macleod [22], and Paterson *et al.* [16]. The reported values of the vapour pressure by Kapur and Macleod are higher than those of Paterson *et al.* by about 25%. No satisfactory explanation of this difference has been found and the data of Paterson *et al.* has been used in this work as Macleod [23] favours this data. The predicted values are however within the uncertainty of the experimental results.

Some preliminary tests conducted with a single and multiple turbulent jet(s) have demonstrated good resolution of fringes obtained with the arrangement described in this work. Typical results obtained are

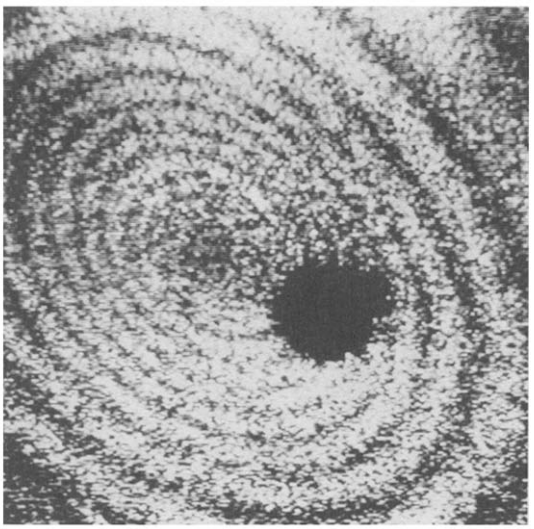

(a)

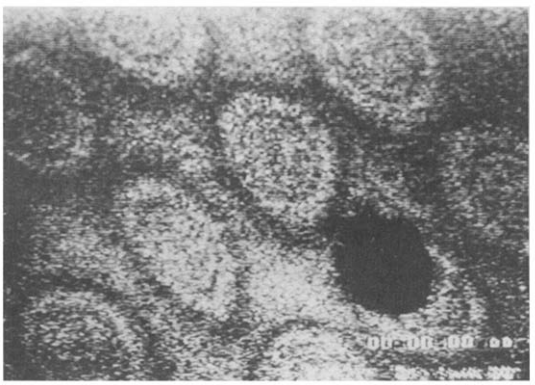

(b)

FIG. 9. Impingement jet interferograms: (a) single turbulent jet ($Re = 14000$, $d = 2.01$ mm, $z/d = 19.8$); (b) multiple turbulent jets ($Q = 6.31$ l min^{-1}, $d = 2.03$ mm, $Px = Py = 30.05$ mm, $z/d = 49.5$).

shown in Fig. 9. Results from the detailed analysis of such fringe patterns will form the subject of future publications.

In the arrangement discussed here the test surface can be attached directly to the optical system so that the beam of light used need not travel through the flow fluid under investigation and thus, optical noise due to density variations of the fluid is avoided. The application of the arrangement in its present form is, however, limited to heat/mass transfer engineering situations which allow the use of a test surface on an optical prism. The size of the test surface used in the arrangement described is also limited by the cost of the optical prism required.

CONCLUSIONS

The novel experimental arrangement described is capable of yielding variation of local mass transfer

over the entire test surface. The arrangement is simple but the manual processing of the interferograms obtained proved to be very time consuming. It is felt that if the processing can be handled automatically with a suitable computer programme, the arrangement can lead to speedy investigation of a host of mass transfer or analogous heat transfer situations.

A knowledge of more accurate values of the vapour pressure of the swelling agent will reduce uncertainty in the measured values of the mass transfer coefficient and in the estimated values of the heat transfer coefficient. With these reductions the arrangement described here will be rendered potentially more useful.

Acknowledgements—The research reported here was carried out in the Department of Mechanical Engineering at Trent Polytechnic. The use of facilities along with the partial financial support of SERC are acknowledged gratefully.

REFERENCES

1. B. L. Button and T. T. Mohamad, Experimental techniques to determine the convective heat transfer coefficients for flat and curved surfaces, *High Temperature Technol.* 163–170 (1983).
2. T. H. Chilton and A. P. Colburn, Mass transfer (absorption) coefficients, *Ind. Engng Chem.* **26,** 1183–1187 (1934).
3. B. L. Button, Jet penetration of a cooling film. Some measurement techniques in heat transfer, Ph.D. thesis, CNAA–Coventry (Lanchester) Polytechnic (1980).
4. N. Macleod and R. B. Todd, The experimental determination of wall–fluid mass transfer coefficients using plasticized polymer surface coatings, *Int. J. Heat Mass Transfer* **16,** 485–504 (1973).
5. D. N. Kapur and N. Macleod, The determination of local mass transfer coefficients by holographic interferometry. 1. General principles: their application and verification for mass transfer measurements at a flat-plate exposed to laminar round jet, *Int. J. Heat Mass Transfer* **17,** 1152–1162 (1974).
6. D. N. Kapur and N. Macleod, The estimation of local heat transfer coefficients for two-dimensional surface roughness elements by holographic interferometry, *Proc. the Engineering Uses of Holography Conf.*, Strathclyde, pp. 615–631 (1975).
7. J. H. Masliyah and T. N. Nguyen, Free convection mass transfer: laminar and turbulent, *Int. J. Heat Mass Transfer* **18,** 1443–1447 (1975).
8. J. H. Masliyah and T. N. Nguyen, Holographic determination of mass transfer due to impinging square jet, *Can. J. Chem. Engng* **54,** 299–304 (1976).
9. J. H. Masliyah and T. N. Nguyen, Experimental study of mass transfer due to an impinging rectangular jet, *Can. J. Chem. Engng* **55,** 156–160 (1977).
10. C. L. Saluja, D. Lampard, N. Hay and I. Burns, The determination of heat transfer coefficients on film-cooled flat surfaces using the swollen polymer technique, *Inst. Chem. Engrs Symp. Ser.* **86,** 893–906 (1984).
11. A. J. Harper and N. Macleod, Hot spots in heat transfer, *Physics Bull.* 13–14 (1978).
12. H. Law and J. H. Masliyah, Mass transfer due to a confined laminar impinging two-dimensional jet, *Int. J. Heat Mass Transfer* **27,** 529–539 (1984).
13. N. G. Hyne and N. Macleod, The use of electronic speckle pattern interferometry for convective mass transfer measurements: studies of transfer due to turbulent air jet impinging on a plane surface, 11th Ann. Res. Meeting, Inst. Chem. Engrs, School of Chem. Engng, University of Bath, pp. 147–152, 9–10 April (1984).
14. R. J. Jones and C. Wykes, *Holographic and Speckle Interferometry*, p. 188. Cambridge University Press, Cambridge (1983).
15. R. Gardon and J. Cobonpue, Heat transfer between a flat plate and jets of air impinging on it, *Proc. 2nd Int. Heat Transfer Conf.*, pp. 454–460 (1962).
16. W. R. Paterson, R. A. Colledge, J. I. MacNab and J. A. Joy, Solid–gas mass transfer measurement by the swollen polymer method: proving of swelling agents, *Int. J. Heat Mass Transfer* **30,** 279–287 (1987).
17. T. Scholtz and O. Trass, Mass transfer in the laminar radial wall jet, *A.I.Ch.E. Jl* 548–554 (1963).
18. M. B. Glauert, *Boundary Layer Research* (Edited by H. Gortler), p. 72. Springer, Berlin (1958).
19. W. H. Schwartz and B. Caswell, Paper presented at the A.I.Ch.E. and C.I.C. Joint Chemical Engineering Conf., Cleveland, Ohio (1961).
20. C. Reid and T. K. Sherwood, *The Properties of Gases and Liquids*, 2nd Edn, p. 523. McGraw-Hill, New York (1966).
21. S. J. Kline and F. A. McClintock, Describing uncertainties in single sample experiments, *Mech. Engng* 3–8 (1953).
22. D. N. Kapur and N. Macleod, Vapour pressure determination for certain high-boiling liquids by holography, *Ind. Engng Chem. Prod. Res. Dev.* **15,** 50–54 (1976).
23. N. Macleod, Private communication (1986).

MESURE IN-SITU DU COEFFICIENT LOCAL DE TRANSFERT DE MASSE UTILISANT LA TECHNIQUE ESPI AVEC UN POLYMERE EXPANSE

Résumé—Un nouveau montage expérimental pour la mesure in-situ d'un coefficient local de transfert de masse est décrit ; il utilise un prisme de verre à angle droit avec un interféromètre électronique à speckle et un polymère expansé. La viabilité du montage est démontrée en considérant le cas d'un jet d'air frappant une surface plane. Les données expérimentales s'accordent avec les prédictions théoriques existantes dans les limites de l'incertitude expérimentale. Des recommandations pratiques sont données pour réduire cette incertitude.

VOLLSTÄNDIGE UNMITTELBARE MESSUNG DES ÖRTLICHEN STOFFÜBERGANGS-KOEFFIZIENTEN MIT HILFE VON ESPI UND DEM "SWOLLEN POLYMER"-VERFAHREN

Zusammenfassung—Es wird eine neuartige Anordnung für die unmittelbare Messung des örtlichen Stoffübergangs-Koeffizienten beschrieben. Hierbei wird ein Glasprisma von Rechteck-Querschnitt mit einem elektronischem "speckle-pattern"-Interferometer (ESPI) und das "swollen polymer"-Verfahren verwendet. Die Tauglichkeit der Anordnung für Stoffübergangs-Untersuchungen wird anhand eines laminaren Luftstrahls, welcher auf eine ebene Oberfläche auftrifft, gezeigt. Die Meßergebnisse stimmen innerhalb der Meßgenauigkeit mit verfügbaren theoretischen Berechnungen überein. Darüberhinaus werden praktische Hinweise zur Verbesserung dieser Meßgenauigkeit gegeben.

ИЗМЕРЕНИЕ ЛОКАЛЬНОГО КОЭФФИЦИЕНТА МАССООБМЕНА СПЕКЛ-МЕТОДОМ

Аннотация—Описана новая экспериментальная установка для измерения локального коэффициента массопереноса с использованием прямоугольной стеклянной призмы с электронным спекл-интерферометром и метода набухшего полимера. Рассмотрено натекание ламинарной струи воздуха на плотную поверхность и показаны возможности установки в получении данных по массопереносу. Данные измерений согласуются с известными теоретическими результатами в пределах ошибки эксперимента. Даны практические рекомендации по уменьшению этой ошибки.